Swansea University
Prifysgol Abertawe

Cronfa
Setting Research Free

Cronfa - Swansea University Open Access Repository

_____

This is an author produced version of a paper published in :
IEEE Transactions on Geoscience and Remote Sensing

Cronfa URL for this paper:
http://cronfa.swan.ac.uk/Record/cronfa30241

_____

Paper:

Hernandez-Clemente, R., Kolari, P., Porcar-Castell, A., Korhonen, L. & Mottus, M. (2016). Tracking the Seasonal
Dynamics of Boreal Forest Photosynthesis Using EO-1 Hyperion Reflectance: Sensitivity to Structural and Illumination
Effects. *IEEE Transactions on Geoscience and Remote Sensing, 54*(9), 5105-5116.
http://dx.doi.org/10.1109/TGRS.2016.2554466

_____

Tracking the Seasonal Dynamics of Forest Photosynthesis using EO-1 Hyperion Reflectance: Sensitivity to Structural and Illumination Effects

First Hernández-Clemente R., Kolari P., Porcar-Castell A., Korhonen L. , Mõttus M.

Abstract—**During the growing season, photosynthesis and growth of boreal forests are regulated by physiological responses to environmental factors. Physiological variations affect the spectral properties of leaves. Linking canopy-level spectral reflectance to leaf-level processes for monitoring forest seasonal physiology using satellite images is hindered by view and illumination effects and variations in canopy structure. To better understand the connection between the two structural levels, we used four narrowband vegetation indices (VIs) derived from Hyperion imagery to track the seasonal dynamics of boreal forest stands: the photochemical reflectance index (PRI) related to the xanthophyll cycle, the red edge (RE) index related to chlorophyll concentration, the carotenoid simple ratio (CSR) related to carotenoid concentration and the normalized difference vegetation index (NDVI) related to fractional cover. As ground truth we used measurements of exposed pine shoot light use efficiency (LUE) and photosynthesis. Over the study period (May to August), LUE and photosynthesis were best correlated with the RE index (R^2=0.71, and R^2=0.63, respectively, p<0.01). The RE index also exhibited the lowest coefficient of variation in association with forest structure. PRI, on the other hand, was affected by canopy structure and observation geometry, and was uncoupled from LUE during the growing season. Our findings demonstrate that the photosynthesis and productivity of boreal forests in the growing season is best tracked using VIs related to total pigment concentration (i.e., chlorophyll).**

Index Terms—**Enter Hyperspectral, Hyperion, Narrowband Vegetation indices, Forest structure, Photosynthesis, Growing season.**

R. Hernández-Clemente is now with the Department of Geography, University of Swansea, SA2 8PP UK (r.hernandez-clemente@swansea.ac.uk).
P. Kolari is with the Department of Physics, P.O. Box 48, FI-00014, University of Helsinki, Finland.
A. Porcar-Castell is with the Department of Forest Sciences, P.O. Box 27 FI-00014, University of Helsinki, Finland.
L. Korhonen is now with.
M. Mottus, is with the Department of Geosciences and Geography, P.O. Box 64, FI-00014, University of Helsinki, Finland.

I. INTRODUCTION

SOLAR energy converted through photosynthesis drives gross primary production (GPP), net ecosystem exchange (NEE) and net primary production (NPP) in green plants [1], [2]. Plants have evolved numerous mechanisms to optimize light absorption, photosynthesis and growth in the face of changing light conditions, temperatures and water status throughout the year [3]. Among such mechanisms, leaf biochemical composition exerts a strong control on photosynthesis [4]. In particular, photosynthetic pigments such as certain xanthophylls contribute to the partitioning of absorbed energy between photochemistry (and thus GPP) and thermal energy. Understanding the seasonal variations in pigment concentrations is crucial for monitoring seasonal and interannual changes in plant functioning [5], [6].

Satellite remote sensing is increasingly used to analyze seasonal changes in boreal forests. A number of studies [7], [8] have found that variations in leaf area index alone (LAI) do not provide a good representation of phenological changes. For instance, the seasonal variations in LAI in coniferous stands are very small with a seasonal course not dynamic enough to characterize the start of growing season in spring [8]. The diagnosis of a range of plant physiological properties and processes implies quantifying not only forest photosynthesizing biomass but also the physiological status of such biomass based on biochemical variables such as leaf chlorophyll a and b concentration (C_{a+b}) or leaf carotenoid concentration (C_{x+c}, the sum of the xanthophyll concentration and the concentration of other carotenes) [9]. Earlier studies have shown a significant decrease of C_{a+b} and C_{x+c} under stress conditions [10], [11], with a simultaneous increase in the ratio of carotenoids to total chlorophylls [12]. Additionally, a special group of carotenoids belonging to the xanthophyll cycle play a photo-protective role, preventing damage from excess light to photosynthetic systems [13]. Dissipation of excess excitation energy by the xanthophyll cycle has been observed under various environmental stresses [14] and in particular, in conifer forest [15].

Several narrowband vegetation indices (VIs) have been proposed to measure canopy biochemistry and plant physiology [16] from a distance. In particular, several studies

have assessed C_{a+b} using narrowband optical indices calculated from spectroscopic data on leaves [17], [18] or the canopy [19]. In forest canopies, one of the most sensitive formulations is the red edge ratio vegetation index (RE=r_{750}/r_{710}, where r is the reflectance factor and the index denotes the wavelength in nanometers) [19], [20]. Vegetation indices sensitive to the total carotenoid concentration have also been analyzed mostly at the leaf level [21], [22]. Moreover, a recent study has demonstrated that VIs related to C_{x+c} behave differently at the leaf and at the canopy level and that a new index – the carotenoid simple ratio index based on bands at 515 and 570 nm, CSR =r_{515}/r_{570} [23] – should be applied at the canopy level. The photochemical reflectance index, PRI=$(r_{531}-r_{570})/(r_{531}+r_{570})$, is commonly considered a proxy for light use efficiency (LUE) because it is affected by carotenoid pigment conversion in what is known as the xanthophyll cycle, leading to a downregulation of carbon assimilation processes. However, also the leaf-level concentrations of other carotenoid pigments on chlorophyll basis have been found to be correlated with the PRI at the seasonal scale [6], [24]. Additionally, this index has been found to be strongly affected by canopy structural effects and illumination conditions [10], [25], [26]. [6] showed that seasonal dynamics in leaf-level PRI in Scots pine foliage are more strongly related to the variation in the carotenoid-to-chlorophyll ratio than to the de-epoxidation level of the xanthophyll cycle. Similar results have recently been obtained in other evergreen conifers [27], corroborating that the PRI is indeed strongly influenced by seasonal changes in this pigment ratio, potentially decoupling it from LUE.

A major challenge in multi-temporal remotely sensed data analysis is acquisition of high-quality image data with adequate temporal, spectral and spatial resolution. Previous studies on seasonal changes have mainly been performed using sensors such as MODIS [28]–[31] and CHRIS/PROBA [32], [33] The low spatial resolution of MODIS (approx. 1 km) is the main limiting factor for accurate estimation of forest status. A better spatial resolution is obtained by EO-1 Hyperion (approx. 30 m), the most widely used spaceborne hyperspectral system. To date, researchers have used Hyperion data to analyze seasonal variations in gap dominance [34], fractional cover [35] and structural and spectral diversity [36]. However, few studies have focused on exploring seasonal biophysical changes in forests using narrowband indices [37]. The main challenges in applying satellite-scale PRI data for retrieving this type of information are the effects of forest structure [10], [38] and viewing geometry [39]. The relative role of each factor and how these factors interact with each other during the growing season needs yet to be determined.

In light of the above, the main objective of this study was to evaluate the photosynthetic seasonal changes of a boreal forest using narrowband VIs calculated from Hyperion image data disentangling the influence of forest structure and viewing angles from the photosynthetic signal. To the best of our knowledge, no quantitative validations have been reported or published so far on narrow band VIs applied to seasonal change analysis.

II. MATERIALS AND METHODS

A. Study site and plot characteristics

The measurement site was located in a boreal forest around the Station for Measuring Ecosystem Atmosphere Relationships (SMEAR II) in Hyytiälä, southern Finland (61˚51'N, 24˚18'E). The station is located inside a 40 to 50-year-old nearly pure pine plot (SMEAR pine plot, or SPP). The stand height of the SPP was approximately 18 m, with an average tree density of 1370 stems (diameter at breast height ≥ 5 cm) per hectare [40].

The growing season in this area typically begins in early May and ends in late August. The snow-covered period typically extends from December to April. The site is located mostly on mineral soils covered by common vascular plant species at ground level [40]. The 30-year average annual precipitation at Hyytiälä is 711 mm and the annual mean temperature is 3.5 ℃ [41]. Seasonal changes were assessed for three consecutive years (2009-2011). During the measurement period, seasonal variations in meteorological variables exhibited a similar pattern according to the data provided by SMEAR II.

B. Hyperion data acquisition and processing

Hyperion acquires visible and near-infrared (VNIR) and shortwave infrared (SWIR) radiation in 220 10-nm-wide contiguous bands in a spectral range from 400 to 2500 nm with a spatial resolution of 30 m. The VNIR and SWIR parts of the spectrum were measured by different spectrometers. The data were delivered by the United States Geological Survey (USGSS) as an L1R product, that is, as scaled at-sensor radiance values including spectral calibration, smearing and echo correction, generation of a bad pixel mask, and alignment of VNIR and SWIR channels [42]. We processed the image by applying a local destriping method [43] and corrected the "smile effect" (i.e., variation in central wavelength and bandwidth across the swath of the sensor) following the "Cross-Track Illumination Correction" procedure [42] in ENVI software (ITT Visual Information Systems, 2006). The image was atmospherically corrected by applying the fast line-of-sight atmospheric analysis of spectral hypercubes (FLAASH) algorithm [44] to top-of-canopy reflectance factors. Atmospheric aerosol levels were estimated using a ground based optical weather sensor and atmospheric water levels were estimated using a CIMEL Electronique 318A sun photometer (data provided by the AErosol RObotic NETwork (AERONET), NASA, 2007) located at the site.

Due to the non-continuous temporal resolution of this satellite and the meteorological conditions, eight cloud-free Hyperion images collected over multiple years (2009-2011) were used to construct a phenological time-series. Although three images had a cloud cover of over 30%, the clouds did not cover the actual study site. We used 2 images acquired by Hyperion in 2011, 5 images acquired in 2010 and 1 image acquired in 2009 (Table 2). Data collection was performed close to nadir (within 6 degrees, 4 images), in the backscattering (2 images) or forward scattering (2 images) directions. All the scenes in this study were 42 km in length and the scenes were centered

on the study site. Both Hyperion time series data and photosynthetic measurements were analyzed in seasonally successive chronological order based on the accumulated growing degree days (GDD). GDD is a temperature-based index frequently used to describe the timing of biological processes [45]. The index was calculated from the meteorological data measured at SMEARII as the sum of all the preceding days in the same year

$$\text{GDD} = \sum \left[\frac{T_{max} + T_{min}}{2} - T_{base} \right] \quad (1)$$

where T_{max} and T_{min} are the daily maximum and minimum temperatures in degrees Celsius, respectively, and T_{base} is the temperature base of +5ºC [46]. Negative values obtained when the daily average temperature was lower than T_{base} were considered zero in the sum in Eq. (1). Time series data was plotted as a function of GDD instead of using the day of the year (DOY) because the seasonal development of photosynthetic activity between years cannot be assumed to be the same.

The Hyperion image series was used to calculate four spectral vegetation indices related to fractional cover [47], chlorophyll a+b concentration [48], carotenoid concentration [23] and light use efficiency [49] (Table 3). To achieve this, the averaged spectral reflectance was extracted from the SPP pure pine plot located at SMEAR II tower.

C. Geometrical effects on PRI

Seasonal variations in PRI can be caused by two different mechanisms: physiological variations of the vegetation and variations in observation conditions. Naturally, it is not possible to separate the two using single view angle medium resolution data such as that measured by Hyperion. Quantifying the first mechanism requires information on the biochemical composition of the canopy which was unavailable at the test site. However, the second mechanism can be modeled using known direct and diffuse sky irradiances if multiple scattering in the canopy is ignored.

According to first-order scattering approximation, PRI of a vegetation canopy measured from a remote sensing platform is related to the leaf spectral albedo $\omega(\lambda)$ as

$$\text{PRI} = \frac{\omega(531)\eta_{\text{PRI}} - \omega(570)}{\omega(531)\eta_{\text{PRI}} + \omega(570)} \quad (2)$$

where η_{PRI} is the spectral distortion factor calculated as

$$\eta_{\text{PRI}} = \frac{\phi(531)\Phi(570)}{\phi(570)\Phi(531)} \quad (3)$$

where $\Phi(\lambda)$ is the downward spectral irradiance on the horizontal top-of-canopy surface, and $\phi(\lambda)$ is the average spectral irradiance on the all-sided surface area of visible leaves [50]. The latter can further be approximated from the diffuse sky irradiance $\Phi_{\text{dif}}(\lambda)$, the direct solar irradiance at top of canopy $\Phi_{\text{dir}}(\lambda)$, and the shadow fraction α_S (i.e., the fraction of visible foliage which is sunlit) as

$$\phi(\lambda) = \frac{1}{4}\Phi_{\text{dif}}(\lambda) + \frac{(1-\alpha_S)G(\theta_S)\Phi_{\text{dir}}(\lambda)}{2\cos\theta_S} \quad (4)$$

where $G(\theta_S)$ is the Ross-Nilson G-function (i.e., the projection of unit foliage in the direction of sun rays) and θ_S is the solar zenith angle. In later calculations we will assume that $G(\alpha_S)=1/2$, that is, the leaves constituting the canopy do not have a preferred orientation. Next, we can define the

difference between the leaf PRI and that of a canopy measured under a specific geometry as

$$\Delta\text{PRI} = \text{PRI} - \text{PRI}_{\text{leaf}} \quad (5)$$

It has been shown that within the natural range of variation of leaf optical properties, the dependence of ΔPRI on $\omega(\lambda)$ is negligible [50]. Thus, ΔPRI in Eq. (5) becomes a function of the spectral distortion factor η_{PRI} only and is fully determined by illumination conditions (i.e., solar zenith angle and the atmospheric conditions determining the fractions of direct and diffuse sky irradiance at the top of canopy) and the shadow fraction α_S. Eqs. (3-5) make it possible to quantify this functional dependence and to retrieve the PRI of an average visible leaf. By definition, leaf-level PRI is free from geometric effects.

In our calculations, we used the average peak growing season atmospheric conditions for Hyytiälä (Table 4) and the 6S atmospheric radiative transfer code [51]. To calculate the shadow fraction α_S, we used the spectral invariants theory [52] and the spectral albedo of pine needles measured in Hyytiälä during peak growing season [53]. The details of the calculations are given in Appendix I.

D. Shoot biochemical constituent & photosynthesis measurements

Seasonal variation in pigment composition was measured between February 2009 and February 2010 at approximately 30-days intervals. The data has been published by [6]. Sixteen youngest fully developed needles were collected from four different branches in three trees (4 needles x 4 branch x 3 tree replicates) located at the SMEAR station. Because the focus of this study was on seasonal processes, measurements were carried out during night time to avoid interference from diurnal acclimation processes. The needle concentrations of total chlorophyll a and b (C_{a+b}) and total carotenoids, xanthophylls and carotenes (C_{x+c}) were determined. The xanthophyll cycle epoxidation state EPS, [54] was calculated as:

$$\text{EPS} = \frac{C_v + 0.5C_a}{C_v + C_a + C_z} \quad (6)$$

where C_v is violaxanthin, C_a anteraxanthin and C_z zeaxanthin foliar concentration. The seasonal course of pigment concentrations were solely plotted to understand the seasonal trend in photosynthetic activity of the vegetation.

The photosynthetic data of exposed shoots were collected from two Scots pine trees during 2009, 2010 and 2011. Carbon flux rates were measured using two shoot chambers, one in each crown, installed horizontally in the top whorls. The needles of the shoots were spread carefully to avoid damage or self-shading. The chambers were almost fully exposed, with only minor shading by neighboring trees in the evening. The tips of the shoots were approximately pointing to the south. A detailed description of the setup has been reported by [55].

Measured shoot LUE and photosynthesis (LUE_m and P_m, respectively) were obtained from shoot chamber data recorded every 30 minutes. Measurements between 11:00 AM and 12:45 PM (local time), corresponding to the time of Hyperion acquisitions, were averaged and used to calculate LUE_m as

$$LUE_m = \frac{P_m}{PPFD_m} \qquad (7)$$

where P_m is the sum of the net photosynthetic assimilation of the shoot per unit of all-sided needle area ($\mu mol\ CO_2\ m^{-2}\ s^{-1}$) and the shoot respiration per unit of all-sided needle area ($\mu mol\ CO2\ m^{-2}\ s^{-1}$), and $PPFD_m$ is the photosynthetic photon flux density ($\mu mol\ photons\ m^{-2}\ s^{-1}$). We used the standard approach of estimating shoot respiration from night measurements of net photosynthesis which were scaled to daytime values assuming a linear dependence between respiration and temperature. Additionally, to smooth out short-term (hours to days) variations in photosynthesis due to instantaneous fluctuations in PPFD and to assess seasonal variations in leaf photosynthetic apparatus, we also calculated the potential LUE (LUE_p) as the average LUE for PPFD <400 $\mu mol\ m^{-2}\ s^{-1}$ from sunrise to 12:45 PM (local time) [6].

E. Shoot photosynthesis model

The two shoot chambers located in the topmost canopy layer are not representative of the whole canopy. To quantify the actual values of LUE_m and P_m of natural (not flattened) shaded and sunlit shoots in all canopy layers in Hyperion's Instantaneous Field of View (IFOV), we computed shoot LUE and photosynthesis using the shoot photosynthesis model described by [55]. The model was parameterized using earlier measurements taken in the same test site and applied using the direct solar and diffuse sky PPFD and meteorological data collected by SMEAR II (Table 1).

No diffuse PPFD data were recorded in 2009 due to a technical failure. This problem affected only one Hyperion acquisition on DOY 181. To fill in the data gap, we calculated the diffuse to total PPFD ratio for the Hyperion acquisition days in 2010. We regressed the ratio linearly against the optical air mass m approximated as $m=1/\cos(\theta_S)$ (for $\theta_S<70°$), where θ_S is the solar zenith angle.

LUE_m and P_m were calculated for a completely shaded and an average exposed shoot. In the absence of multiple scattering within the canopy, the average diffuse sky PPFD on both the shaded and exposed shoots visible to a sensor can be approximated as ½ of the diffuse downwelling PPFD at the top of the canopy [50]. For the exposed shoot, a direct solar PPFD component calculated on a surface perpendicular to sunrays was added from top-of-canopy measurements.

The signal scattered by both types of shoots into the IFOV of Hyperion depends on two factors: the fraction of each type of foliage in the IFOV, and the radiance produced by the shoots. The fraction of shaded and sunlit foliage in the IFOV was quantified by the shadow fraction α_s and its complement $1-\alpha_s$, respectively. The radiance produced by a shoot was assumed to be proportional to its intercepted irradiance. Finally, we normalized the relative contributions of sunlit and shaded shoots in the Hyperion signal to add to unity and used the resulting normalized weights to calculate the Hyperion-Weighted Measured LUE and photosynthesis (LUE_{hwm} and P_{hwm}, respectively). As the irradiance conditions were only available for photosynthetically active radiation, LUE_{hwm} and P_{hwm} were only compared to the index using wavelengths in the visible part of the spectrum, the PRI.

III. RESULTS

A. Seasonal variation in photosynthetic conditions and narrowband VIs

The growing season GDD dynamics are shown in Fig. 1 for 2009, 2010 and 2011. The earliest start date of the growing season (GDD>0) was DOY 100 (mid-April) in 2011, and the latest end of growing season date was DOY 295 (end of October, also in 2011), with the most rapid increase in GDD at around DOY 210 (end of July). At the end of the season, the average GDD of the three years was 1346 degree-days (Fig. 1). The beginning of the growing season triggered the strongest variations in pigment concentration over the season (Fig. 2): most variations took place during the accumulation of the first 100 degree-days. The general trend of the vegetation was a rapid increase in chlorophyll concentration and a slight decrease in that of total carotenoids between the end of April (114 degree-days) and the end of August (1200 degree-days), breaking down from this date until the next spring. Fig. 2 also shows a fast increase of the EPS during the accumulation of the first 100 degree-days, after which the EPS remained relatively stable up to the accumulation of 1200 degree-days, when it broke down until the next spring. A clear seasonal cycle was present in C_{a+b}, C_{a+b}/C_{x+c} and EPS with coefficients of variation of 0.19, 0.19 and 0.35 respectively. The time span covered by Hyperion acquisitions included variations in C_{a+b} and C_{x+c}, and a monotonic decrease in the C_{a+b}/C_{x+c} ratio. By contrast, only small variations occurred in the EPS during the period covered by Hyperion images, as the strongest changes in these pigments took place before the first available image (DOY=125) (Fig. 2).

The strongest variations in shoot LUE and photosynthesis happened during the accumulation of the first 200 degree-days (DOY 125-DOY 181) (Fig. 3). The maximum values of exposed shoot LUE measured during 2009, 2010 and 2011 were recorded in August (around DOY 250) after accumulating 950 degree-days. Photosynthesis measured in the exposed shoots showed a rising trend over the growing season (Fig. 3).

The seasonal courses of VIs followed a somewhat different pattern depending on the VI analyzed. The most obvious changes were observed in the RE displaying a consistent increasing trend throughout the growing season (Fig. 4). In contrast, NDVI, PRI and CSR displayed seasonal variations with large fluctuations. NDVI exhibited an increasing trend while the PRI and CSR decreased over the season.

B. Relationships between LUE, photosynthesis and VIs

Table 5 lists the coefficients of variation between the Hyperion-measured VIs and the measured shoot light use efficiency (LUE_m) and photosynthesis (P_m). Among the four VIs, the relationship between RE and LUE_m yielded the highest coefficient of determination ($R^2=0.71$, $p<0.01$). The modeled Hyperion-weighed LUE_{hwm} had an even higher coefficient of determination with RE, $R^2=0.82$ ($p<0.01$) (Fig. 5). In contrast, the other VIs, NDVI, CSR and PRI, yielded

$R^2=0.24$, $R^2=0.06$ and $R^2=0.29$, respectively, with LUE_m. The highest coefficient of determination for measured exposed shoot photosynthesis were found between the measured P_m and RE, yielding a coefficient of determination of $R^2=0.63$ (p<0.05). Non-significant relationships (p>0.05) were found between P_m and the other three VIs. The linear equations fitted between RE, and LUE_m and LUE_p are presented in Fig. 5. The highest coefficient of determination between a shoot photosynthesis parameter and a VI were found for the measured LUE_p and RE, $R^2=0.89$ (p<0.01) (Fig. 5). It is noteworthy that the Hyperion-measured PRI yielded non-significant relationships (p>0.05) with the shoot LUE values, LUE_m, LUE_p (Table 5) and LUE_{hwm}.

C. Solar illumination effects on VIs

The canopy-level PRI was strongly correlated with the shadow fraction α_S ($R^2=0.79$, p<0.01, Fig. 6a). Similarly, the spectral distortion factor and thus ΔPRI (i.e., the difference between the canopy- and leaf-level PRI) depended mostly on α_S (Fig. 6b). The leaf-level PRI calculated as PRI – ΔPRI and thus corrected for geometric effects yielded a slightly higher coefficient of determination ($R^2=0.32$) with LUE_m (Fig. 6c) compared to canopy PRI ($R^2=0.29$, Table 5). Similarly to the canopy-level index, the trend between the leaf-level PRI and LUE was negative. However, the dependence of PRI on LUE_m lacked statistical significance for both levels. In addition, Fig. 6d shows that the exposed shoot LUE_m was significantly and strongly correlated with ΔPRI, a purely geometric quantity ($R^2=0.68$, p<0.01). PRI was strongly and significantly correlated with two characteristics of illumination and view geometry: solar zenith angle ($R^2=0.66$, p<0.05) (Fig. 7a) and scattering angle ($R^2=0.60$, p<0.05) (Fig. 7b). In contrast, non-significant relationships (p>0.05) were observed between RE and both solar zenith angle (Fig. 7c) and scattering angle (Fig. 7d).

IV. DISCUSION

After the first 15 accumulated degree-days, most of the photosynthetic indicators analyzed in this study showed a rapid variation indicating the start of the growing season (Fig. 1). Exposed shoot LUE and photosynthesis changed hand in hand with chlorophyll pools (Figs. 2 and 3). The differences between the LUE_m and P_m curves for the three years can mostly be attributed to varying light levels. This is especially evident for the year 2011 when lower P_m levels around 600 GDD are accompanied by a simultaneous increase in LUE_m, a situation characteristic to a cloudy spell. It is noteworthy that with the exception of LUE_m for 2011, LUE_m, P_m and C_{a+b} peaked in late summer, as did also RE – the only VI strongly correlated with seasonal changes in the three physiological parameters. Thus, photosynthetic capacity reached its maximum in August. This gives a hypothetical chance to decouple it from the effects of solar angle with a maximum in the end of June.

PRI was relatively constant at GDD<500 (Fig. 4) with a possible decrease in the last two Hyperion images at GDD>800. However, the last two images were the only ones taken in 2011, thus the decrease can also be attributed to interannual variation. The other three indices showed a stable trend, either an increasing one (NDVI, RE), or a slightly decreasing one (CSR). The biggest fluctuation in all four indices plotted against GDD is DOY 181. This is the only image from 2009 used in the analysis. Excluding this data point, the curves for RE and NDVI become even more smooth.

It is clear that, as expected, use of GDD cannot completely remove the interannual variations in the time series of VIs. However, we have mostly used it for qualitative analysis of forest phenology and illustrative purposes. The results regarding the indices and shoot photosynthesis which are discussed below were obtained directly from satellite and in situ measurements and are not affected by the interannual differences in the timing of forest development.

LUE is lower under high light conditions than with moderate light (e.g., [56]). Thus, the measured LUE_m was expectedly lower than the potential LUE_p measured under low light conditions (Fig. 5). As LUE_p is independent from light conditions, we expected it to be correlated with reflectance at wavelengths where slowly changing pigments, such as chlorophyll, dominate. Indeed, it was correlated with RE more strongly than LUE_m ($R^2=0.89$ and $R^2=0.71$, respectively) (Fig.5). This finding indicates that, at the spectral and spatial resolutions of Hyperion, the optical signal of photosynthetic capacity of the foliage is dominated by basic foliar biochemistry.

The correlation between the measured exposed shoot LUE_m and canopy-level PRI for the SMEAR II plot was negative and moderately strong (Table 4), yet statistically insignificant. The use of the ΔPRI to convert from canopy- to leaf-level PRI somewhat increased the coefficient of determination. This, together with the strong correlation between LUE_p and RE, corroborates the representativeness of the two shoot chambers and the overall validity of our approach.

Previous studies in Hyytiälä that found a clear seasonal change in leaf-level PRI measured at the leaf level with a dark-acclimation clip (Porcar-Castell et al., 2012). That study showed PRI to be strongly correlated with LUE during most of the year but decoupled in early spring under strong stress when the foliage was deeply downregulated. The main challenge in relating LUE measurements with PRI estimated from satellite-measured reflectance is the dependence of this VI on illumination conditions, which create an apparent variation in the index. Our study corroborated earlier findings [25], [39], [57] on this topic (Figs. 6 and 7): PRI is weakly correlated with the view nadir angle (data not shown; eastward off-nadir viewing directions yield a higher PRI value), strongly correlated with the solar zenith angle (smaller zenith angles yield a higher PRI) and scattering angle, and most strongly correlated with the shadow fraction (a smaller PRI for a larger shadow fraction).

The accuracy of the conversion from canopy PRI to shoot PRI contains several simplifying assumptions (e.g., no multiple scattering in the canopy, simplified scattering phase

function). Nevertheless, the uncertainties involved in our computations cannot change the unexpected negative nature of the PRI–LUE relationship (PRI decreases with increasing LUE) for both structural levels: it is known that multiple scattering within structured vegetation increases the absolute value of PRI [58] and therefore cannot change the directionality of the PRI-LUE relationship. For the shadow fraction values occurring for Hyperion acquisitions in Hyytiälä, ΔPRI was always positive (Fig. 6) and converting from canopy to needle level only enhanced the negative dependence between PRI and LUE.

At the leaf level, a decrease in PRI denotes downregulation of the photosynthetic apparatus, mediated either via interconversion of the xanthophyll cycle pigments (diurnal scale) or via adjustments in carotenoid:chlorophyll ratios (seasonal scale) [22], [6]. Either way, a positive relationship between PRI and LUE is to be expected on these physiological grounds. The anomalous negative relationship between PRI and LUE – and also between PRI and α_S (Fig. 6) – obtained from Hyperion data indicates that the mechanism causing the observed variation in the PRI between May and August in a boreal forest does not have a simple physiological explanation. More likely, it is a result of other changes in average needle optical properties (e.g., in the proportional area of first-year needles) or a physical process (e.g., an artefact of atmospheric correction).

The shoot photosynthesis model allowed us to estimate the photosynthetic downregulation at the time of Hyperion acquisitions under mostly cloudless skies. For sunlit shoots, LUE was between 45% and 65% of that of shaded shoots with no clear seasonal trend. Lack of a trend indicates that the shoots adapted to environmental light conditions: its photosynthetic efficiency (i.e., LUE under shaded non-saturating light conditions) increased until the summer solstice, thus compensating for the increase in solar irradiance. Also, the period covered by Hyperion images (May – August) excludes the strongest seasonal changes in the spring. There were no extreme weather events during the study period that could have caused stress and excess photosynthetic downregulation on ordinary sunny spring and summer days and break the balance between light conditions and needle biochemistry.

In this study, we could not untangle the different factors affecting the PRI of a structured vegetation canopy. Besides carotenoid absorption, this index is at the canopy level affected by canopy structure, the amount and spectrum of incident blue sky radiation, understory and soil reflectance, and possibly also by the specular reflectance from leaf surface [50]. Unfortunately, obtaining cloudless hyperspectral imagery in the boreal region is rather an exception than a rule. Extending the dynamic range of PRI by increasing the number and the time span of satellite observations would be difficult and would lead to additional problems such as partial snow cover or very low sun angles.

V. CONCLUSION

Our results demonstrate that seasonal (May to August) monitoring of the dynamics of photosynthetic activity is not feasible with PRI, a vegetation index directly related to leaf-level changes in LUE as this index is highly correlated with observation geometry and forest structure. Over the growing season, PRI showed an unexpected negative relationship with both shadow fraction and exposed shoot LUE. In contrast, the chlorophyll index RE=r_{750}/r_{710} showed a significant correlation with exposed shoot LUE and photosynthesis while being independent from observation geometry and forest structure. The seasonal courses of boreal forest photosynthetic status during the growing season (characterized by the LUE of its sunlit shoots), is best monitored with remotely sensed chlorophyll concentration, at least in the absence of extreme events (e.g. droughts, pest attacks): of the VIs analyzed here, the RE chlorophyll index was the one most correlated with both measured and modeled shoot LUE and was also insensitive to view geometry

APPENDIX

According to the spectral invariants theory [52], the following relationship holds universally for sufficiently closed vegetation canopies for wavelengths between 710 and 790 nm:

$$\frac{\text{BRF}(\lambda)}{\omega(\lambda)} = p\text{BRF}(\lambda) + \rho \qquad (A1)$$

where p and ρ are spectrally invariant parameters. The parameters were determined from Hyperion image data by fitting a straight line to BRF$(\lambda)/(\omega(\lambda)$ plotted against BRF(λ) for 710nm≤λ≤790nm. The value of $\omega(\lambda)$ can be generated using the PROSPECT leaf optical properties model [59], [60]. The PROSPECT-generated reference leaf albedo is connected to all actual transformed leaf albedos via relationships similar to Eq. (A1) in this spectral interval. For the pine needles measured in Hyytiälä [53] we obtained

$$\frac{\omega_{pine}}{\omega_{PROSPECT}} = 0.352\omega_{pine} + 0.648 \qquad (A2)$$

Next, we assumed that the canopy-leaving radiance of a closed canopy equals the average radiance scattered by the visible leaves,

$$\text{BRF}(\lambda) = \omega(\lambda)\frac{\phi(\lambda)}{\Phi(\lambda)} \qquad (A3)$$

As diffuse sky radiation can be ignored in the red edge spectral region but not the radiation scattered several times in the canopy, we can break the leaf-level irradiance $\phi(\lambda)$ into that produced by multiple scattering inside the canopy (ϕ_d) and the direct beam

$$\phi(\lambda) = \phi_d(\lambda) + \frac{1}{2}(1 - \alpha_S)\frac{\Phi(\lambda)G(\theta_S)}{\cos\theta_S} \qquad (A4)$$

where the factor ½ on the right hand side of Eq. (A4) comes from the fact that only one side of a leaf is illuminated by the direct beam. After inserting the leaf-level irradiance $\phi(\lambda)$ from Eq. (A4) into Eq. (A3) and dividing the result by $\omega(\lambda)$, we obtain

$$\frac{\text{BRF}(\lambda)}{\omega(\lambda)} = \frac{\phi_d(\lambda)}{\Phi(\lambda)} + \frac{1}{2}(1 - \alpha_S)\frac{G(\theta_S)}{\cos\theta_S} \qquad (A5)$$

The first term on the RHS of Eq. (A5) is a function of $\omega(\lambda)$

satisfying the condition $\lim_{\omega \to 0} \frac{\phi_{d(\lambda)}}{\Phi(\lambda)} = 0$. It is clear that the second term, on the other hand, is a geometric constant. Thus, by comparison with Eq. (A1) we obtain that

$$\rho = \frac{1}{2}(1 - \alpha_S)\frac{G(\theta_S)}{\cos \theta_S} \qquad (A6)$$

Assuming, as previously, $G(\theta_S)=1/2$, we obtain for the shadow fraction

$$\alpha_S = 1 - 4 \cos \theta_S \, \rho \qquad (A7)$$

REFERENCES

[1] X. Xiao, Q. Zhang, B. Braswell, S. Urbanski, S. Boles, S. Wofsy, B. Moore III, and D. Ojima, "Modeling gross primary production of temperate deciduous broadleaf forest using satellite images and climate data," *Remote Sens. Environ.*, vol. 91, no. 2, pp. 256–270, May 2004.

[2] W. Yuan, S. Liu, G. Yu, J.-M. Bonnefond, J. Chen, K. Davis, A. R. Desai, A. H. Goldstein, D. Gianelle, F. Rossi, A. E. Suyker, and S. B. Verma, "Global estimates of evapotranspiration and gross primary production based on MODIS and global meteorology data," *Remote Sens. Environ.*, vol. 114, no. 7, pp. 1416–1431, Jul. 2010.

[3] M. Stitt, "Plant Growth: Basic Principles and Issues Relating to the
Optimization of Biomass Production and Composition as a
Feedstock for Energy," Feb. 2013.

[4] S. Evain, J. Flexas, and I. Moya, "A new instrument for passive remote sensing: 2. Measurement of leaf and canopy reflectance changes at 531 nm and their relationship with photosynthesis and chlorophyll fluorescence," *Remote Sens. Environ.*, vol. 91, no. 2, pp. 175–185, May 2004.

[5] D. W. Lee, J. O'Keefe, N. M. Holbrook, and T. S. Feild, "Pigment dynamics and autumn leaf senescence in a New England deciduous forest, eastern USA," *Ecol. Res.*, vol. 18, no. 6, pp. 677–694, 2003.

[6] A. Porcar-Castell, J. I. Garcia-Plazaola, C. J. Nichol, P. Kolari, B. Olascoaga, N. Kuusinen, B. Fernández-Marín, M. Pulkkinen, E. Juurola, and E. Nikinmaa, "Physiology of the seasonal relationship between the photochemical reflectance index and photosynthetic light use efficiency," *Oecologia*, vol. 170, no. 2, pp. 313–323, Oct. 2012.

[7] J. R. Miller, H. P. White, J. M. Chen, D. R. Peddle, G. McDermid, R. A. Fournier, P. Shepherd, I. Rubinstein, J. Freemantle, R. Soffer, and E. LeDrew, "Seasonal change in understory reflectance of boreal forests and influence on canopy vegetation indices," *J. Geophys. Res.*, vol. 102, no. D24, p. 29475, Dec. 1997.

[8] M. Rautiainen, J. Heiskanen, and L. Korhonen, *Seasonal changes in canopy leaf area index and MODIS vegetation products for a boreal forest site in central Finland*, vol. 17. Helsinki, Finland: Finnish Environment Institute, 2012.

[9] G. A. Blackburn, "Hyperspectral remote sensing of plant pigments," *J. Exp. Bot.*, vol. 58, no. 4, pp. 855–867, Nov. 2006.

[10] R. Hernández-Clemente, R. M. Navarro-Cerrillo, L. Suarez, F. Morales, and P. J. Zarco-Tejada, "Assessing structural effects on PRI for stress detection in conifer forests," *Remote Sens. Environ.*, vol. 115, no. 9, pp. 2360–2375, Sep. 2011.

[11] M. Lippert, K.-H. Häberle, K. Steiner, H.-D. Payer, and K.-E. Rehfuess, "Interactive effects of elevated CO2 and O3 on photosynthesis and biomass production of clonal 5-year-old Norway spruce [Picea abies (L.) Karst.] under different nitrogen nutrition and irrigation treatments," *Trees*, vol. 10, no. 6, pp. 382–392, Aug. 1996.

[12] J. A. Moran, A. K. Mitchell, G. Goodmanson, and K. A. Stockburger, "Differentiation among effects of nitrogen fertilization treatments on conifer seedlings by foliar reflectance: a comparison of methods," *Tree Physiol.*, vol. 20, no. 16, pp. 1113–1120, Oct. 2000.

[13] H. Scheer, "The Pigments," in *Light-Harvesting Antennas in Photosynthesis*, B. R. Green and W. W. Parson, Eds. Springer Netherlands, 2003, pp. 29–81.

[14] A. J. Young, D. Phillip, A. V. Ruban, P. Horton, and H. A. Frank, "The xanthophyll cycle and carotenoid-mediated dissipation of excess excitation energy in photosynthesis : Pure and Applied Chemistry," *Pure Appl. Chem.*, vol. 69, no. 10, pp. 2125–2130, 2009.

[15] J. J. Peguero-Pina, F. Morales, J. Flexas, E. Gil-Pelegrín, and I. Moya, "Photochemistry, remotely sensed physiological reflectance index and de-epoxidation state of the xanthophyll cycle in Quercus coccifera under intense drought," *Oecologia*, vol. 156, no. 1, pp. 1–11, May 2008.

[16] G. A. Blackburn, "Hyperspectral remote sensing of plant pigments," *J. Exp. Bot.*, vol. 58, no. 4, pp. 855–867, Mar. 2007.

[17] G. le Maire, C. François, K. Soudani, D. Berveiller, J.-Y. Pontailler, N. Bréda, H. Genet, H. Davi, and E. Dufrêne, "Calibration and validation of hyperspectral indices for the estimation of broadleaved forest leaf chlorophyll content, leaf mass per area, leaf area index and leaf canopy biomass," *Remote Sens. Environ.*, vol. 112, no. 10, pp. 3846–3864, Oct. 2008.

[18] R. Main, M. A. Cho, R. Mathieu, M. M. O'Kennedy, A. Ramoelo, and S. Koch, "An investigation into robust spectral indices for leaf chlorophyll estimation," *ISPRS J. Photogramm. Remote Sens.*, vol. 66, no. 6, pp. 751–761, Nov. 2011.

[19] P. J. Zarco-Tejada, J. R. Miller, T. L. Noland, G. H. Mohammed, and P. H. Sampson, "Scaling-up and model inversion methods with narrowband optical indices for chlorophyll content estimation in closed forest canopies with hyperspectral data," *IEEE Trans. Geosci. Remote Sens.*, vol. 39, no. 7, pp. 1491–1507, Jul. 2001.

[20] Q. Zhang, X. Xiao, B. Braswell, E. Linder, F. Baret, and B. Moore III, "Estimating light absorption by chlorophyll, leaf and canopy in a deciduous broadleaf forest using MODIS data and a radiative transfer model," *Remote Sens. Environ.*, vol. 99, no. 3, pp. 357–371, Nov. 2005.

[21] A. A. Gitelson, Y. Zur, O. B. Chivkunova, and M. N. Merzlyak, "Assessing Carotenoid Content in Plant Leaves with Reflectance Spectroscopy¶," *Photochem. Photobiol.*, vol. 75, no. 3, pp. 272–281, 2002.

[22] J. Penuelas, I. Filella, and J. Gamon, "Assessment of Photosynthetic Radiation-Use Efficiency with Spectral Reflectance," *New Phytol.*, vol. 131, no. 3, pp. 291–296, Nov. 1995.

[23] R. Hernández-Clemente, R. M. Navarro-Cerrillo, and P. J. Zarco-Tejada, "Carotenoid content estimation in a heterogeneous conifer forest using narrow-band indices and PROSPECT + DART simulations," *Remote Sens. Environ.*, vol. 127, pp. 298–315, Dec. 2012.

[24] I. Filella, J. Peñuelas, L. Llorens, and M. Estiarte, "Reflectance assessment of seasonal and annual changes in biomass and CO2 uptake of a Mediterranean shrubland submitted to experimental warming and drought," *Remote Sens. Environ.*, vol. 90, no. 3, pp. 308–318, Apr. 2004.

[25] T. Hilker, F. G. Hall, N. C. Coops, J. G. Collatz, T. A. Black, C. J. Tucker, P. J. Sellers, and N. Grant, "Remote sensing of transpiration and heat fluxes using multi-angle observations," *Remote Sens. Environ.*, vol. 137, pp. 31–42, Oct. 2013.

[26] L. Suárez, P. J. Zarco-Tejada, J. A. J. Berni, V. González-Dugo, and E. Fereres, "Modelling PRI for water stress detection using radiative transfer models," *Remote Sens. Environ.*, vol. 113, no. 4, pp. 730–744, Apr. 2009.

[27] C. Y. S. Wong and J. A. Gamon, "Three causes of variation in the photochemical reflectance index (PRI) in evergreen conifers," *New Phytol.*, Nov. 2014.

[28] J. Heiskanen, M. Rautiainen, P. Stenberg, M. Mõttus, V.-H. Vesanto, L. Korhonen, and T. Majasalmi, "Seasonal variation in {MODIS} {LAI} for a boreal forest area in Finland," *Remote Sens. Environ.*, vol. 126, no. 0, pp. 104 – 115, 2012.

[29] X. Huang and M. A. Friedl, "Distance metric-based forest cover change detection using MODIS time series," *Int. J. Appl. Earth Obs. Geoinformation*, vol. 29, pp. 78–92, Jun. 2014.

[30] J. Pisek, M. Rautiainen, J. Heiskanen, and M. Mõttus, "Retrieval of seasonal dynamics of forest understory reflectance in a Northern European boreal forest from MODIS BRDF data," *Remote Sens. Environ.*, vol. 117, pp. 464–468, Feb. 2012.

[31] H. Tang, K. Yu, O. Hagolle, K. Jiang, X. Geng, and Y. Zhao, "A cloud detection method based on a time series of MODIS surface reflectance images," *Int. J. Digit. Earth*, vol. 6, no. sup1, pp. 157–171, Dec. 2013.

[32] S. Stagakis, N. Markos, O. Sykioti, and A. Kyparissis, "Monitoring canopy biophysical and biochemical parameters in ecosystem scale

using satellite hyperspectral imagery: An application on a Phlomis fruticosa Mediterranean ecosystem using multiangular CHRIS/PROBA observations," *Remote Sens. Environ.*, vol. 114, no. 5, pp. 977–994, May 2010.

[33] J. Verrelst, M. E. Schaepman, B. Koetz, and M. Kneubühler, "Angular sensitivity analysis of vegetation indices derived from CHRIS/PROBA data," *Remote Sens. Environ.*, vol. 112, no. 5, pp. 2341–2353, May 2008.

[34] J. R. Foster, P. A. Townsend, and C. E. Zganjar, "Spatial and temporal patterns of gap dominance by low-canopy lianas detected using EO-1 Hyperion and Landsat Thematic Mapper," *Remote Sens. Environ.*, vol. 112, no. 5, pp. 2104–2117, May 2008.

[35] J. P. Guerschman, M. J. Hill, L. J. Renzullo, D. J. Barrett, A. S. Marks, and E. J. Botha, "Estimating fractional cover of photosynthetic vegetation, non-photosynthetic vegetation and bare soil in the Australian tropical savanna region upscaling the EO-1 Hyperion and MODIS sensors," *Remote Sens. Environ.*, vol. 113, no. 5, pp. 928–945, May 2009.

[36] J. C. White, C. Gómez, M. A. Wulder, and N. C. Coops, "Characterizing temperate forest structural and spectral diversity with Hyperion EO-1 data," *Remote Sens. Environ.*, vol. 114, no. 7, pp. 1576–1589, Jul. 2010.

[37] P. K. E. Campbell, E. M. Middleton, K. J. Thome, R. F. Kokaly, K. F. Huemmrich, D. Lagomasino, K. A. Novick, and N. A. Brunsell, "EO-1 Hyperion Reflectance Time Series at Calibration and Validation Sites: Stability and Sensitivity to Seasonal Dynamics," *IEEE J. Sel. Top. Appl. Earth Obs. Remote Sens.*, vol. 6, no. 2, pp. 276–290, Apr. 2013.

[38] M. F. Garbulsky, J. Peñuelas, J. Gamon, Y. Inoue, and I. Filella, "The photochemical reflectance index (PRI) and the remote sensing of leaf, canopy and ecosystem radiation use efficiencies: A review and meta-analysis," *Remote Sens. Environ.*, vol. 115, no. 2, pp. 281–297, Feb. 2011.

[39] L. S. Galvão, D. A. Roberts, A. R. Formaggio, I. Numata, and F. M. Breunig, "View angle effects on the discrimination of soybean varieties and on the relationships between vegetation indices and yield using off-nadir Hyperion data," *Remote Sens. Environ.*, vol. 113, no. 4, pp. 846–856, Apr. 2009.

[40] H. Ilvesniemi, J. Levula, R. Ojansuu, P. Kolari, L. Kulmala, J. Pumpanen, S. Launiainen, T. Vesala, and N. Eero, "Long-term measurements of the carbon balance of a boreal Scots pine dominated forest ecosystem," *Boreal Environ. Res.*, vol. 14, pp. 731–753, 2009.

[41] P. Pirinen, H. Simola, J. Aalto, J.-P. Kaukoranta, P. Karlsson, and R. Ruuhela, *Tilastoja Suomen ilmastosta 1981 - 2010*. Ilmatieteen laitos, 2012.

[42] D. L. B. Jupp, B. Datt, T. R. Mcvicar, T. G. Van Niel, J. S. Pearlman, J. L. Lovell, and E. King, "Improving the analysis of hyperion red-edge index from an agricultural area," in *SPIE proceedings series*, 2003, pp. 78–92.

[43] B. Datt, T. R. McVicar, T. G. Van Niel, D. L. B. Jupp, and J. S. Pearlman, "Preprocessing eo-1 hyperion hyperspectral data to support the application of agricultural indexes," *IEEE Trans. Geosci. Remote Sens.*, vol. 41, no. 6, pp. 1246–1259, Jun. 2003.

[44] R. Beck, "EO-1 User Guide v. 2.3." University of Cincinnati, Ohio., 15-Jul-2003.

[45] G. S. McMaster and W. W. Wilhelm, "Growing degree-days: One equation, two interpretations," *Agric. For. Meteorol.*, vol. 87, no. 4, pp. 291–300, 1997.

[46] H. Salminen, "The effect of temperature on height growth of Scots pine in northern Finland," *Lämpötilan vaikutus männyn pituuskasvuun Pohjois-Suomessa*, Nov. 2009.

[47] J. W. Rouse Jr., R. H. Haas, J. A. Schell, and D. W. Deering, "Monitoring Vegetation Systems in the Great Plains with Erts," *NASA Spec. Publ.*, vol. 351, p. 309, 1974.

[48] P. J. Zarco-Tejada, J. R. Miller, J. Harron, B. Hu, T. L. Noland, N. Goel, G. H. Mohammed, and P. Sampson, "Needle chlorophyll content estimation through model inversion using hyperspectral data from boreal conifer forest canopies," *Remote Sens. Environ.*, vol. 89, no. 2, pp. 189–199, Jan. 2004.

[49] J. A. Gamon, L. Serrano, and J. S. Surfus, "The photochemical reflectance index: an optical indicator of photosynthetic radiation use efficiency across species, functional types, and nutrient levels," *Oecologia*, vol. 112, no. 4, pp. 492–501, Nov. 1997.

[50] M. Mõttus, T. L. H. Takala, P. Stenberg, Y. Knyazikhin, B. Yang, and T. Nilson, "Diffuse sky radiation influences the relationship between canopy PRI and shadow fraction," *ISPRS J. Photogramm. Remote Sens.*, vol. 105, pp. 54–60, Jul. 2015.

[51] E. F. Vermote, N. El Saleous, C. O. Justice, Y. J. Kaufman, J. L. Privette, L. Remer, J. C. Roger, and D. Tanré, "Atmospheric correction of visible to middle-infrared EOS-MODIS data over land surfaces: Background, operational algorithm and validation," *J. Geophys. Res. Atmospheres*, vol. 102, no. D14, pp. 17131–17141, 1997.

[52] Y. Knyazikhin, P. Lewis, M. I. Disney, P. Stenberg, M. Mõttus, M. Rautiainen, R. K. Kaufmann, A. Marshak, M. A. Schull, P. Latorre Carmona, V. Vanderbilt, A. B. Davis, F. Baret, S. Jacquemoud, A. Lyapustin, Y. Yang, and R. B. Myneni, "Reply to Townsend et al.: Decoupling contributions from canopy structure and leaf optics is critical for remote sensing leaf biochemistry.," *Proc Natl Acad Sci U A*, vol. 110, no. 12, p. E1075–?, Mar. 2013.

[53] P. Lukeš, P. Stenberg, M. Rautiainen, M. Mõttus, and K. M. Vanhatalo, "Optical properties of leaves and needles for boreal tree species in Europe," *Remote Sens. Lett.*, vol. 4, no. 7, pp. 667–676, Jul. 2013.

[54] S. S. Thayer and O. Björkman, "Leaf Xanthophyll content and composition in sun and shade determined by HPLC," *Photosynth. Res.*, vol. 23, no. 3, pp. 331–343, Mar. 1990.

[55] P. Kolari, H. K. Lappalainen, H. Hänninen, and P. Hari, "Relationship between temperature and the seasonal course of photosynthesis in Scots pine at northern timberline and in southern boreal zone," *Tellus B*, vol. 59, no. 3, pp. 542–552, 2007.

[56] N. P. A. Hürner, G. Öquist, and F. Sarhan, "Energy balance and acclimation to light and cold. Trends Plant Sci 3:224-230," *Trends Plant Sci.*, vol. 3, no. 6, pp. 224–230, 1998.

[57] C. V. M. Barton and P. R. J. North, "Remote sensing of canopy light use efficiency using the photochemical reflectance index: Model and sensitivity analysis," *Remote Sens. Environ.*, vol. 78, no. 3, pp. 264–273, Dec. 2001.

[58] M. Mottus and M. Rautiainen, "Scaling PRI Between Coniferous Canopy Structures," *IEEE J. Sel. Top. Appl. Earth Obs. Remote Sens.*, vol. 6, no. 2, pp. 708–714, Apr. 2013.

[59] J.-B. Feret, C. François, G. P. Asner, A. A. Gitelson, R. E. Martin, L. P. R. Bidel, S. L. Ustin, G. le Maire, and S. Jacquemoud, "PROSPECT-4 and 5: Advances in the leaf optical properties model separating photosynthetic pigments," *Remote Sens. Environ.*, vol. 112, no. 6, pp. 3030–3043, Jun. 2008.

[60] S. Jacquemoud and F. Baret, "PROSPECT: A model of leaf optical properties spectra," *Remote Sens. Environ.*, vol. 34, no. 2, pp. 75–91, Nov. 1990.

Rocío Hernández-Clemente holds a degree in agricultural engineering from the School of Agricultural Engineering and Forestry, University of Córdoba, Spain, and an International PhD degree accredited by the Department of Forestry, University of Córdoba, Spain. She has been a contract faculty member for remote sensing at the University of Helsinki, Finland. Her specific lines of research are focused on the analysis of high-resolution hyperspectral data to estimate leaf biochemical and canopy biophysical variables through leaf and canopy radiative transfer modeling. She currently holds an Intra-European Fellowship for Career Development (IEF) at University of Swansea, UK.

Pasi Kolari received a PhD degree in plant biology at the University of Helsinki. He has published 67 peer-reviewed scientific articles on forest-atmosphere interactions, main focus being in the ecophysiology of trees, gas exchange measurements and integration of small-scale CO2 exchange processes into long-term carbon balances of forest

stands. Currently he works as post-doc researcher at Department of Physics, University of Helsinki. His main tasks are data curation and database administration for SMEAR research stations and work for greenhouse gas observation infrastructure ICOS. He is the principal investigator (PI) of Värriö ICOS ecosystem station.

Albert Porcar-Castell received his BSc degree in Forest Industry Engineering from the University of Lleida, Spain, in 1998. He moved to Finland in 1999 to study Forest Ecology and Silviculture and completed his MSc and PhD degrees at the University of Helsinki in 2002 and 2008, respectively. Alongside his studies he worked occasionally as consultant for forest private sector. He is currently a principal investigator and Academy Research Fellow at the Department of Forest Sciences in the University of Helsinki. His Lab (Optics of Photosynthesis Laboratory) investigates the mechanisms and processes that link chlorophyll fluorescence and spectral reflectance to photosynthesis. Dr. Porcar-Castell has conducted pioneering work on the study of the seasonal acclimation of photosynthesis using chlorophyll fluorescence and the photochemical reflectance index
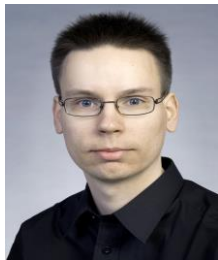
Lauri Korhonen received the D.Sc. degree in forestry from the University of Eastern Finland (UEF), Joensuu, Finland, in 2011. He is currently a researcher with the School of Forest Sciences, UEF. His two main research themes are measurements of forest canopy properties and forest inventory with airborne lidar data.

Matti Mõttus received the M.Sc. degree in physics and the Ph.D. degree in environmental physics, from the University of Tartu, Tartu, Estonia, in 2000 and 2004, respectively. He has worked with the Tartu Observatory, Tartu, Estonia and the University of Helsinki, Helsinki, Finland. He is currently an Academy of Finland Research Fellow with the Department of Geosciences and Geography, University of Helsinki, Helsinki, Finland. His current research interests include imaging spectroscopy and radiative transfer in vegetation canopies.